Carbon 145 (2019) 452–461

Contents lists available at ScienceDirect

Carbon

journal homepage: www.elsevier.com/locate/carbon

Piezoelectric and piezoresistive behavior of unmodified carbon fiber

Xiang Xi, D.D.L. Chung*

Composite Materials Research Laboratory, Department of Mechanical and Aerospace Engineering, University at Buffalo, The State University of New York, Buffalo, NY, 14260-4400, USA

ARTICLE INFO

Article history:
Received 10 October 2018
Received in revised form
19 December 2018
Accepted 13 January 2019
Available online 14 January 2019

ABSTRACT

This work reports the piezoelectric and piezoresistive behavior of unmodified unpoled continuous 12 K/24 K carbon fiber (polyacrylonitrile-based, tensile modulus 240 GPa, electrical resistivity $1.6 \times 10^{-5}\ \Omega\,m$). The first report of the effect of stress on the permittivity of carbon fiber is provided. Under elastic tension (strain $\leq$0.041%, stress $\leq$100 MPa), the piezoelectric coupling coefficient d_{33} is 5×10^{-8} pC/N, with the stress-induced electric field increase ($\leq$103%) contributing 2×10^{-8} pC/N, the stress-induced permittivity increase also contributing 2×10^{-8} pC/N, and the stress-induced field-permittivity increase contributing 9×10^{-9} pC/N. Due to the stress, the relative permittivity (2 kHz) increases by $\leq$ 150% ($\leq$31700) and the DC resistivity decreases by $\leq$ 44% ($\geq 9 \times 10^{-6}\ \Omega\,m$). The strong negative piezoresistivity, with stress-dependent gage factor ranging from −410 (<0.02% strain) to −1900 (>0.02% strain), is attributed to (i) the low modulus and consequent feasibility of preferred orientation increase as the strain/stress increases, and (ii) the low strain and the tendency for high strain (prior work) to cause damage that increases the resistivity, thereby reducing the negative piezoresistivity. Permittivity increase and resistivity decrease result from the increased movement of the charge carriers. All effects are monotonic and reversible, enable piezoelectricity/piezoresistivity-based self-sensing, and are independent of the sizing or the number of fibers per tow.

1. Introduction

Piezoelectric behavior is attractive for numerous applications, particularly sensing and mechanical energy harvesting utilizing the direct piezoelectric effect, and actuation utilizing the converse (inverse) piezoelectric effect. This behavior is described by the piezoelectric coupling coefficient and is most prominently exhibited by certain ceramic materials (such as lead zirconotitanate, abbreviated PZT). It is advantageous to render a structural material the piezoelectric function, since the structural material is available in large sizes, as needed for large-scale energy harvesting. In contrast, the assembly and electrical wiring of piezoceramic elements of small sizes to form a structure of substantial size would be cumbersome and the resulting structure would be expected to be inadequate in the mechanical ruggedness.

Piezoresistive behavior refers to the change in the electrical resistivity with strain. If the resistivity increases with strain, the phenomenon is said to be positive piezoresistivity. If the resistivity decreases with strain, the phenomenon is said to be negative piezoresistivity. Whether it is positive or negative, piezoresistivity enables resistance-based sensing of strain or stress. It is described by the gage factor, which is defined as the fractional change in resistance per unit strain. In contrast, the direct piezoelectric effect enables sensing that is based on measuring the capacitance or electric field.

The piezoresistive or piezoelectric behavior enables the carbon fiber to be self-sensing (i.e., being able to sense itself without any attached or embedded sensor). Compared to sensing based on attached or embedded sensors, self-sensing is advantageous in the low cost, high durability, large sensing volume and absence of mechanical property loss.

Polymer-matrix composites with continuous carbon fibers are attractive for lightweight structures, such as airframe, due to their combination of low density, high strength and high elastic modulus [1]. In order to render the piezoelectric function to these composites, zinc oxide nanowires, which are piezoelectric, have been grown on the carbon fibers [2]; this approach suffers from the high cost of the nanowire growth and the difficulty of handling the modified carbon fibers to form a composite with a high volume fraction of the carbon fiber. Another approach involves the addition

* Corresponding author.
E-mail address: ddlchung@buffalo.edu (D.D.L. Chung).
URL: http://alum.mit.edu/www/ddlchung

https://doi.org/10.1016/j.carbon.2019.01.044
0008-6223/

of PZT piezoelectric particles as a filler to the matrix of the continuous carbon fiber polymer-matrix composite [3]; this approach suffers from the reduction of the fracture energy due to the filler addition. These problems would be greatly alleviated if the carbon fibers themselves (without modification) are piezoelectric.

Another disadvantage of the use of modified carbon fibers for providing piezoelectricity is that existing composite structures do not involve modified carbon fibers. The use of modified carbon fibers requires the composite structures to be new, thus greatly limiting the applicability of the technology.

This paper is directed at investigating the inherent piezoelectric and piezoresistive behavior of unmodified continuous carbon fiber without poling. Poling is disadvantageous, as it is followed by depoling and hence the need for repoling. In addition, poling requires a high electric field, the application of which to a large structure tends to be difficult. The inherent piezoelectric behavior was first reported by Mischok et al., in 2018 [4], who measured the voltage output upon impact, but did not report the piezoelectric coupling coefficient or the mechanism of the piezoelectric effect.

The inherent piezoresistive behavior of carbon fiber was first reported by Conor and Owston in 1969 [5]. The reported gage factor is positive and ranges from 0.7 to 1.7.

The fractional change in resistance ($\delta R/R$) relates to the fractional change in resistivity ($\delta\rho/\rho$), the longitudinal strain ($\delta\ell/\ell$) and the Poisson's ratio (ν) according to the equation [6].

$$\delta R/R = \delta\rho/\rho + (\delta\ell/\ell)\,(1 + 2\nu), \quad (1)$$

for the case in which the material is isotropic in the two transverse directions, i.e., $\nu_{12} = \nu_{13}$. This case applies to the carbon fiber. For carbon fiber, $\nu = 0.27$ [7]. Based on Eq. (1) and the abovementioned ν value, the gage factor is equal to 1.54 if $\delta\rho/\rho = 0$. If the gage factor is less than 1.54, $\delta\rho/\rho < 0$, which means that the piezoresistivity is negative. Hence, the piezoresistivity reported by Conor and Owston is negative.

In 1971, Berg et al. [7,8], reported that the gage factor is 0.6 for low-modulus carbon fibers and is negative for high-modulus fibers, i.e., negative piezoresistivity for all the fibers. In 1997, Wang and Chung [9] reported gage factor around 1.9, thus also indicating negative piezoresistivity. On the other hand, Blazewicz et al., in 1997 [10] reported gage factor values ranging from −8.9 to +2.8, such that the high-modulus fibers tend to have negative values of the gage factor and the low-modulus fibers tend to have positive values of the gage factor. In particular, Blazewicz et al. reported that the gage factor is +0.82 (i.e., negative piezoresistivity) for PAN 2000 fiber, which has modulus 240 GPa (equal to the modulus of the fibers used in this work). In 2019, Yao et al. [11] reported gage factor values ranging from −3.97 to 1.39 (i.e., negative piezoresistivity for all these gage factor values), such that the high-modulus fiber tested has a negative value of the gage factor. Thus, all prior reports of piezoresistivity in carbon fibers pertains to negative piezoresistivity.

This work is partly directed at providing a thorough characterization of the inherent piezoelectric behavior of carbon fiber. For this purpose, the capacitance and electric field outputs of the direct piezoelectric effect are measured for various values of the tensile stress. In addition, the permittivity and resistivity (two fundamental material properties) are measured for various values of the tensile stress in order to shed light on the scientific origin of the piezoelectric effect.

There is no prior work on the effect of stress on the permittivity of carbon fiber. This effect provides a means of capacitance-based stress sensing. Furthermore, it contributes to the direct piezoelectric behavior. Therefore, this work is partly directed at investigating for the first time the effect of stress on the permittivity of carbon fiber.

It was previously reported that the piezoresistivity of carbon fiber depends on the strain, at least for some of the fiber types [5,8]. All of the prior work on the piezoresistivity of carbon fiber pertains to relatively high strains, $>1 \times 10^{-3}$ [5,8,11], $>4 \times 10^{-3}$ [9], and $>1 \times 10^{-4}$ [10]. Low strains are important for numerous applications, particularly those related to microelectromechanical devices and nanotechnology. This work is thus partly directed at investigating the piezoresistivity at low strains, as low as 4×10^{-5}.

The objectives of this work are three-fold and pertain to the direct piezoelectric effect, the piezoresistive effect and the effect of stress on the permittivity of carbon fibers. All three effects relate to the effect of stress on the electrical and dielectric behavior of carbon fibers, and they impart self-sensing ability to the fibers.

2. Experimental methods

2.1. Materials

Two types of carbon fiber (type A and type B) are studied in this work. They are both continuous polyacrylonitrile (PAN) based carbon fiber, as provided by Teijin (S. Korea). Both types are high-strength standard-modulus aerospace grade carbon fiber. The two corresponding types differ only in the composition of the sizing (epoxy vs. polyurethane), the amount of the sizing (sizing level at 1.3% vs. 1.0%, according to the manufacturer), the number of fibers per tow (12,000 vs. 24,000) and the tow width (3.76 mm vs. 5.82 mm). A larger tow width results from a higher number of fibers per tow. The comparative study of these two fiber types is aimed at investigating the effect (if any) of the sizing, the number of fibers per tow and the fiber-fiber interaction on the mechanical, electrical and electromechanical behavior. For both types, the fiber diameter is 7.0 μm and the tensile modulus is 240 GPa [12]. The small differences in the density, tensile strength, tensile ductility and electrical resistivity, as described below, are primarily due to the difference in the sizing.

Type A is Tenax-E HTS45 E23 12 K 800tex, with 12,000 fibers per tow, 1.3% sizing based on epoxy resin, density 1.77 g/cm^3, linear mass density 800 tex (without sizing), tensile strength 4500 MPa, and tensile ductility 1.9% [12]. The electrical resistivity is 1.6×10^{-5} Ω m [13]. Type A is identical to the type used in our prior work on the permittivity in the absence of stress [14].

Type B is Tenax-E STS40 F13 24 K 1600tex, with 24,000 fibers per tow, 1.0% sizing based on polyurethane, density 1.78 g/cm^3, linear mass density 1600 tex (without sizing), tensile strength 4300 MPa, and tensile ductility 1.8% [12]. The resistivity is 1.5×10^{-5} Ω m [15].

2.2. Mechanical testing method

The mechanical testing system is stepper motor-driven (Mark-10 ESM303, Mark-10 Corp., Copiague, NY), providing force up to 1.5 kN. The force is increased at the rate 90 N/min. The tensile stress is given by the force divided by the cross-sectional area of all the fibers in the tow.

The specimen is a single tow, with the tow axis along the direction of capacitance/voltage/resistance measurement. The specimen is adhered at its two ends by using epoxy adhesive on a cardboard (thickness 0.715 mm) that is in the shape of a picture frame (Fig. 1). The two sides of the picture frame parallel to the specimen are cut just before the start of tensile testing, which is performed along the tow axis. Due to the limited strength of the adhesive joint between the tow and the cardboard, the maximum stress used in this work is about 110 MPa.

In case of stress-strain curve determination, an attached

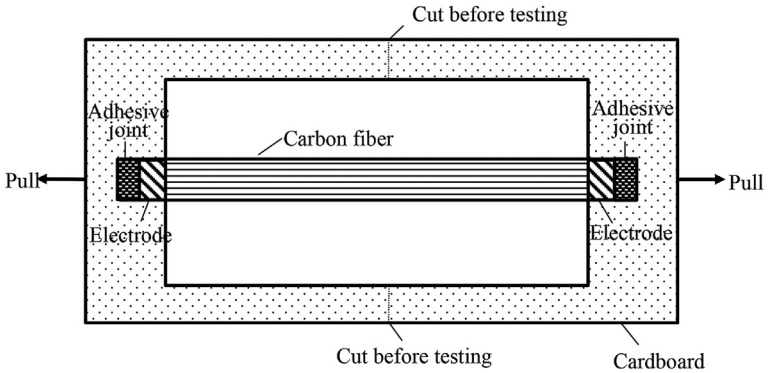

(a)

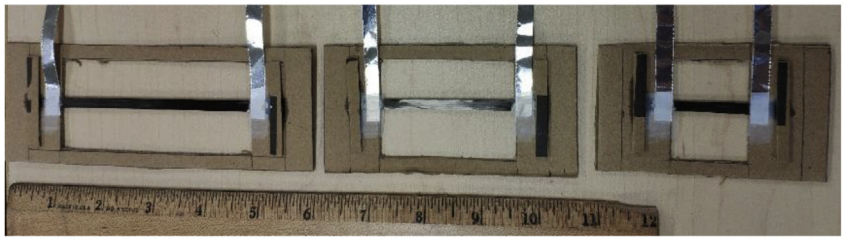

(b)

Fig. 1. Testing configuration. (a) Carbon fiber tow mounting for capacitance/voltage measurement during tensile testing. (b) Photograph showing mounted carbon fiber tow (Type A) of three lengths (L, 2L and 3L), along with a ruler with the main divisions in inches. (A colour version of this figure can be viewed online.)

resistive strain gage is used to measure the strain of the tow. The strain gage is adhered to the tow by using epoxy resin, which penetrates the tow, as enabled by sonication of the tow at 50 °C for 25 min immediately after the resin application, followed by room-temperature curing under a small pressure for 1 day. The procedure for attaching the two ends of the tow to the cardboard is the same.

2.3. Capacitance and permittivity measurement methods

The method of capacitance and permittivity measurement is an extension of the method of prior work for the fiber under no stress [12]. It involves a dielectric film in the form of 6 layers of double-sided adhesive tape (thickness 0.077 mm per layer, thickness 0.46 mm for the 6 layers combined) between the specimen and each electrode, as necessitated by the fact that an LCR meter used for capacitance measurement is not designed for measuring the capacitance of a low-resistance material system. The electrode is household aluminum foil attached to each end of the specimen near the end by using the dielectric film (Fig. 1(a)).

The method also involves the decoupling of the interfacial capacitance from the volumetric capacitance, as achieved by testing the fiber tow at three different lengths (L, 2L and 3L), where L ~ 31.75 mm, with the exact value measured for each specimen. In this context, the interface is that between the specimen and electrode, including the dielectric film.

The capacitance is measured using an LCR meter (Instek LCR-816 High Precision LCR Meter). The frequency is 2.000 kHz, because this is the highest frequency provided by the meter and a frequency in the kHz range is commonly available and widely used. The error in the capacitance measurement is ±0.01 pF. The capacitance reported is that for the equivalent circuit of capacitance and resistance in series. This circuit model is intended to indicate the setting used in the meter, rather than the method of analysis. The AC voltage (0.300, 0.600 or 0.900 V) is adjusted so that the AC electric field (9.45 V/m) is the same for the different inter-electrode distances.

The measured capacitance C_m is given by

$$1/C_m = 1/C + 2/C_i, \tag{2}$$

where C is the specimen volumetric capacitance, and C_i is the interfacial capacitance for one interface. The C relates to the relative permittivity κ of the carbon fiber by the equation

$$C = \varepsilon_o \kappa A/l, \tag{3}$$

where ε_o is the permittivity of free space (8.85×10^{-12} F/m), A is the cross-sectional area of all of the fibers in the tow, and l is the length of the specimen between the two electrodes in the direction of the capacitance measurement (i.e., L, $2L$ or $3L$). Combining Eqs. (2) and (3) gives

$$1/C_m = l/(\varepsilon_o \kappa A) + 2/C_i. \tag{4}$$

Based on Eq. (4), a plot of $1/C_m$ vs. l gives a line of slope equal to $1/(\varepsilon_o \kappa A)$. Hence, from the slope, κ is obtained. For each stress value, κ is determined using this method.

2.4. Electric field output measurement method

The voltage output is measured using the same specimen configuration as Fig. 1, except that the dielectric film is replaced by silver paint. The DC voltage is measured using a precision digital multimeter (Keithley Model 2002). For the relevant voltage range (within 200 mV), the resolution is 1 nV and the input resistance exceeds 100 GΩ [16]. The electric field is the voltage divided by the distance between the proximate edges of the electrodes.

2.5. Resistivity measurement method

The DC electrical resistivity is measured using the same specimen configuration as Fig. 1, except that the dielectric film is replaced by silver paint. The method also involves the decoupling of the interfacial resistance from the volumetric resistance, as achieved by testing the fiber tow at three different lengths (L, 2L and 3L), where L ~ 31.75 mm, with the exact value measured for each specimen. In this context, the interface is that between the specimen and electrode, including the silver paint.

For measurement using two electrodes, the two interfacial resistances and the specimen volumetric resistance are three resistors in series electrically. Hence, the measured resistance R_m is given by

$$R_m = R + 2R_i, \tag{5}$$

where R is the specimen volumetric resistance, and R_i is the interfacial resistance for one interface. The R relates to the resistivity ρ of the specimen by the equation

$$R = \rho l/A, \tag{6}$$

where A is the cross-sectional area of all the fibers in the tow, and l is the length of the specimen between the two electrodes (i.e., L, $2L$ or $3L$).

Combining Eqs. (5) and (6) gives

$$R_m = \rho l/A + 2R_i, \tag{7}$$

Based on Eq. (7), a plot of R_m vs. l gives a line of slope equal to ρ/A. Hence, from the slope, ρ is obtained.

The applied tensile stress of up to 97.4 MPa causes a tensile strain up to 0.041%, according to the modulus of 240 GPa. This strain causes the resistivity obtained by assuming zero strain at various stress values to be overestimated by up to 0.041%, which is negligible. The contribution due to the Poisson's effect is even more negligible.

The DC resistance is measured using a precision digital multimeter (Keithley Model 2002) operating in the two-wire mode. For the range of resistance of this work, the resolution is 100 nΩ and the current provided by the meter is 7.2 mA [16].

3. Results and discussion

3.1. Tensile behavior

The tensile modulus determined in this work up to a stress of 110 MPa and a strain of 0.046% is (239.2 ± 0.6) GPa and (238.6 ± 0.3) GPa for type A fiber and type B fiber, respectively. These values are equal within the experimental error, indicating that the differences in sizing and in the number of fibers per tow do not affect the modulus. These modulus values are consistent with the value of 240 GPa provided by the manufacturer [12].

The stress-strain curve is not up to fracture, but is up to a stress of about 110 MPa, which corresponds to a strain of about 0.046% (Fig. 2). For either fiber type, the curve is linear, except that the slope increases very slightly with increasing strain above about 0.03%. For type A fiber, the modulus for the initial linear part (up to a stress of 39 MPa or a strain of 0.016%) is 239.07 ± 0.18 GPa, which is close to the value of 239.2 ± 0.6 GPa obtained from the entire stress-strain curve shown in Fig. 2. For type B fiber, the modulus for the initial linear part (up to a stress of 34 MPa or a strain of 0.015%) is 236.48 ± 0.09 GPa, which is close to but slightly lower than the value of 238.6 ± 0.3 GPa obtained from the entire stress-strain curve. The slope (modulus) increase in the high-stress region is clearer for type B fiber than type A fiber. The modulus increase is consistent with prior reports of the modulus increasing with increasing tensile stress, i.e., non-Hookean behavior [17–19]. The modulus increases at low stresses up to 330 MPa, particularly significantly at low stresses up to 100 MPa [17]. The modulus increase due to the stress was reported in the prior work for two types of carbon fiber that exhibit modulus 380 and 270 GPa [17]. The modulus increase is attributed to the increase in the degree of axial preferred orientation of the carbon layers and the crystallite deformation being increasingly constrained as the tensile stress increases [18].

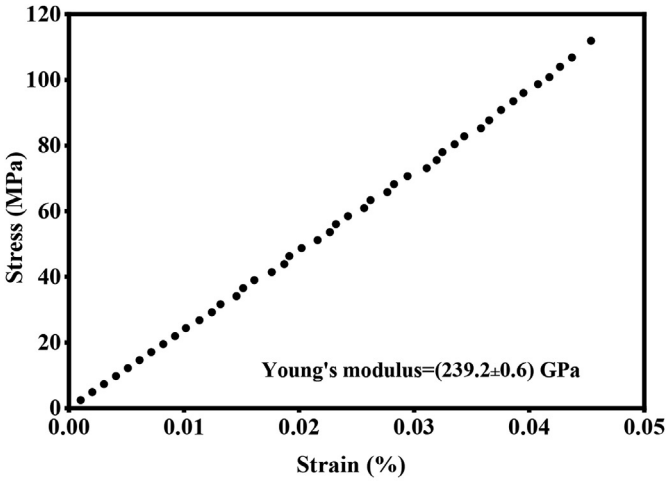

(a)

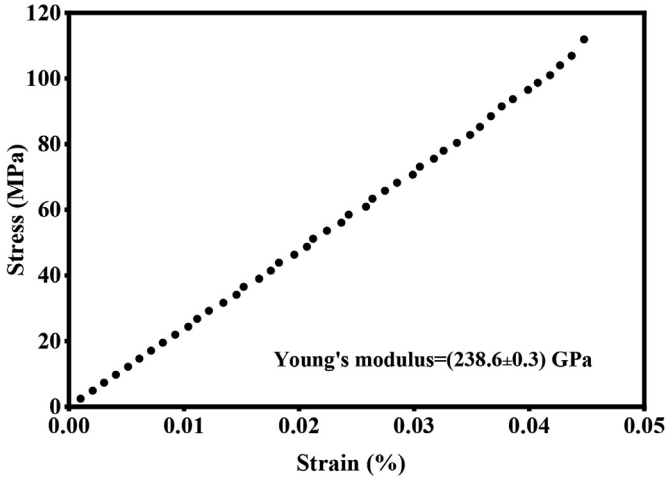

(b)

Fig. 2. Tensile stress-strain curve up to about 110 MPa. (a) Type A fiber. (b) Type B fiber.

3.2. Electrical behavior in the absence of stress

In the absence of stress, the electrical resistivity is $(1.55 \pm 0.02) \times 10^{-5}\,\Omega\,m$ [14] and $(1.57 \pm 0.01) \times 10^{-5}\,\Omega\,m$ for type A fiber and type B fiber, respectively. With consideration of the experimental error, these values are equal, indicating that the differences in sizing and in the number of fibers per tow do not affect the resistivity. Moreover, these values are consistent with the

values mentioned in Sec. 2.1.

In the absence of stress, the relative permittivity is 12515 ± 741 [14] and 12519 ± 215 for type A fiber and type B fiber, respectively. These values are equal within the experimental error, indicating that the differences in sizing and in the number of fibers per tow do not affect the permittivity.

3.3. Electrical behavior in the presence of stress

Fig. 3 shows that the measured capacitance C_m increases monotonically with increasing stress during loading, whether the carbon fiber tow is of length L, 2L or 3L. The capacitance change is totally reversible upon unloading. The C_m increases gently with increasing stress below 80 MPa and increases more abruptly as the stress increases beyond 80 MPa. The increase in distance between the electrodes as the tensile stress increases would have been expected to decrease C_m. The observed increase in C_m is due to the increase in κ, which is determined in this work and described below.

For every stress value, the plot of $1/C_m$ vs. distance l according to Eq. (4) is highly linear. Fig. 4 gives representative plots. The error in κ is obtained by considering the range of values of the slope. Fig. 5 and Table 1 show that κ increases monotonically with increasing stress. The behavior is similar for type A and type B fibers. The κ increases gently with increasing stress below 80 MPa and increases more abruptly as the stress increases beyond 80 MPa. The dependence of κ on stress (Fig. 5) mirrors that of C_m on stress (Fig. 3). This similarity supports the notion that the observed increase in C_m is due to the increase in κ. The fractional increase in κ due to the stress is up to (150 ± 12)% and (152 ± 5)% for type A fiber and type B fiber, respectively. This means that the fractional increase in κ due to the stress is the same for the two fiber types. The reversibility of the increase in κ is indicated by the reversibility of the increase in the capacitance (Fig. 3).

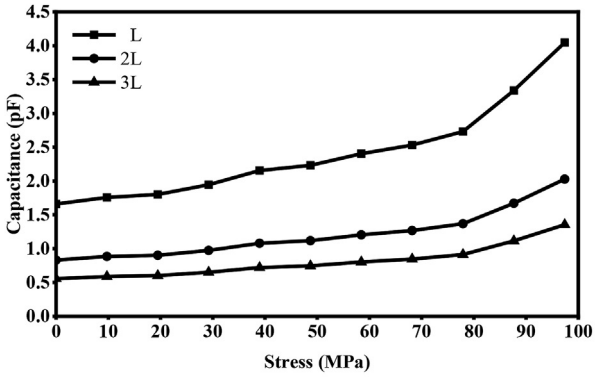

(a)

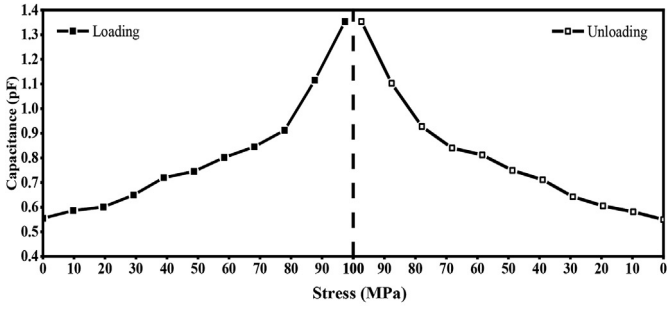

(b)

Fig. 3. Effect of tensile stress on the measured capacitance C_m for type A. (a) Capacitance during loading of carbon fiber tow of lengths L, 2L and 3L. (b) Comparison of the effect during loading (left panel) and subsequent unloading (right panel). The specimen length between the two electrodes is 95.25 mm.

Fig. 6 shows that the electric field output increases monotonically and reversibly with increasing stress. The behavior is similar for type A and type B fibers. The fractional change in electric field due to the stress is up to (110 ± 8)% and (103 ± 4)% for type A fiber and type B fiber, respectively. This means that the fractional increase in electric field is essentially the same for the two fiber types.

The change in polarization ΔP due to a change in stress is given by Ref. [6].

$$\Delta P = (\kappa - 1)\,(\Delta Q/A) + (\Delta\kappa)\,(Q/A) + \Delta\kappa\,\Delta Q/A, \tag{8}$$

where ΔQ is the change in the stored charge due to the change in stress $\Delta\sigma$, $\Delta\kappa$ is the change in κ due to the change in stress, κ is the relative permittivity in the absence of the change in stress, Q is the stored charge in the absence of the change in stress, and A is the area of the capacitor. The first term on the right side of Eq. (8) describes the classical piezoelectric effect that is due to the change in Q; the second term describes the non-classical piezoelectric effect that is due to the change in κ; the third term describes the non-classical piezoelectric effect that is due to both the change in κ and the change in Q. Thus, the polarization changes in response to both the change in Q and the change in κ.

The longitudinal piezoelectric coupling coefficient d (i.e., d_{33}) is given by

$$d = \Delta P/\Delta\sigma. \tag{9}$$

If the piezoelectric effect were solely and classically due to the change in Q (i.e., the first term on the right side of Eq. (8)), d is given by Ref. [6].

$$d = (\kappa - 1)\,\varepsilon_0\,\Delta E/\Delta\sigma, \tag{10}$$

where ΔE is the change in electric field due to the change in stress $\Delta\sigma$. By using the approximately linear part of the curve in Fig. 6 and using the zero-stress relative permittivity (Table 1), d is obtained as $(1.7 \pm 0.3) \times 10^{-8}$ pC/N and $(2.1 \pm 0.2) \times 10^{-8}$ pC/N for type A fiber and type B fiber, respectively. This means that d based on Eq. (10) is essentially the same for the two fiber types. The d is small in spite of the large value of κ. The small value of d is due to the large value of $\Delta\sigma$ and the small value of ΔE.

If the piezoelectric effect were solely due to the change in κ (i.e., the second term on the right side of Eq. (8)),

$$d = (\Delta\kappa)\,(Q/A)\,/\,\Delta\sigma = (\Delta\kappa/\Delta\sigma)\,\varepsilon_0 E, \tag{11}$$

where E is the electric field in the absence of the change in stress. By using the approximately linear part of the curve in Fig. 5 and using the zero-stress electric field of 1.28×10^{-5} V/m and 1.25×10^{-5} V/m for type A fiber and type B fiber, respectively, d is obtained as $(1.3 \pm 0.2) \times 10^{-8}$ pC/N and $(1.8 \pm 0.3) \times 10^{-8}$ pC/N for type A fiber and type B fiber, respectively. This means that the d value based on Eq. (11) is slightly higher for type B than type A.

If the piezoelectric effect were solely due to the last term on the right side of Eq. (8),

$$d = (\Delta\kappa/\Delta\sigma)\,\varepsilon_0\,\Delta E, \tag{12}$$

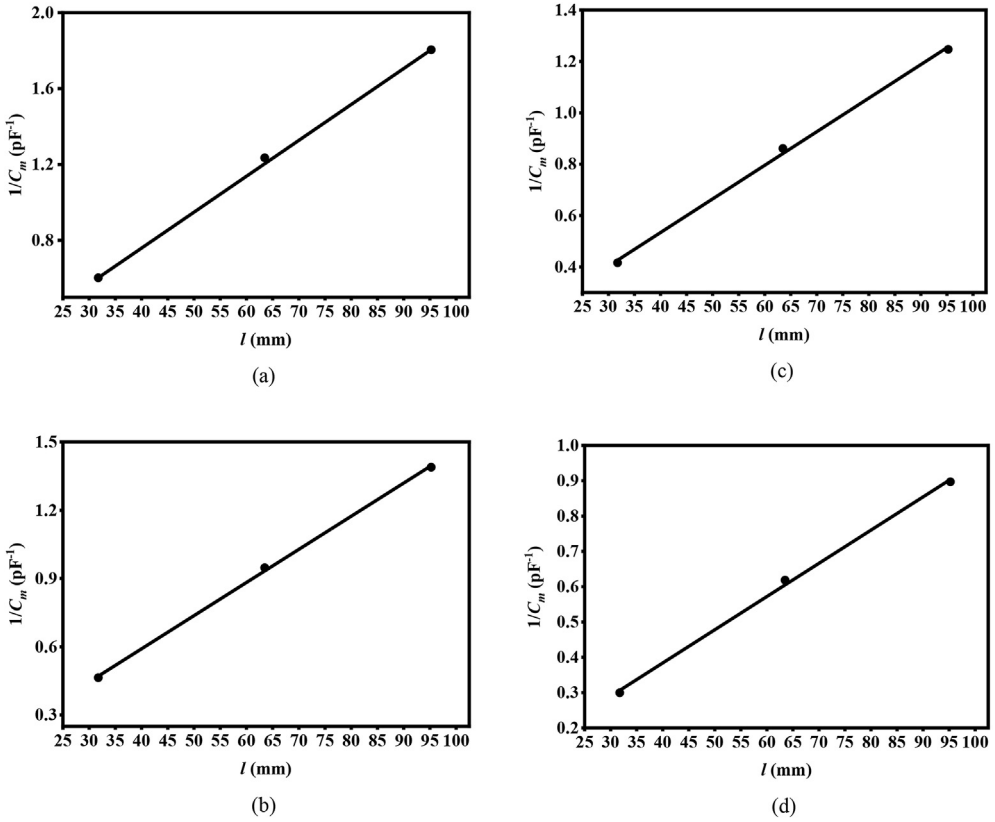

Fig. 4. Plot of $1/C_m$ vs. distance l according to Eq. (4) for type A fiber. (a) Stress = 0. (b) Stress = 39.0 MPa. (c) Stress = 58.4 MPa. (d) Stress = 87.7 MPa.

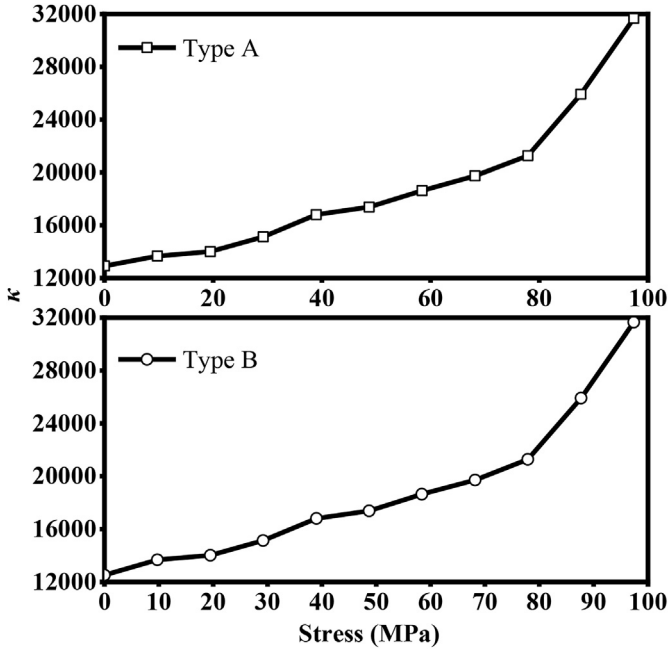

Fig. 5. Effect of the tensile stress on the relative permittivity κ of carbon fiber during loading.

which gives d values of $(9.3 \pm 0.6) \times 10^{-9}$ pC/N and $(8.6 \pm 0.5) \times 10^{-9}$ pC/N for type A fiber and type B fiber, respectively. This means that the d value based on Eq. (12) is essentially equal for the two types of fiber.

Table 1
Relative permittivity (2 kHz) and electrical resistivity (DC) of carbon fibers at various tensile stress values.

Stress (MPa)	Relative permittivity		Resistivity (10^{-5} Ω m)	
	Type A	Type B	Type A	Type B
0	12515 ± 741	12519 ± 215	1.55 ± 0.02	1.57 ± 0.01
9.74	13665 ± 559	13678 ± 361	1.54 ± 0.08	1.55 ± 0.03
19.5	14008 ± 722	14016 ± 365	1.51 ± 0.01	1.52 ± 0.02
29.2	15126 ± 917	15134 ± 298	1.48 ± 0.04	1.48 ± 0.02
39.0	16811 ± 825	16805 ± 236	1.46 ± 0.06	1.46 ± 0.04
48.7	17385 ± 973	17382 ± 251	1.43 ± 0.04	1.44 ± 0.02
58.4	18629 ± 669	18642 ± 318	1.36 ± 0.07	1.38 ± 0.03
68.2	19738 ± 1005	19712 ± 199	1.28 ± 0.06	1.28 ± 0.05
77.9	21265 ± 746	21271 ± 216	1.12 ± 0.03	1.11 ± 0.04
87.7	25927 ± 558	25914 ± 239	1.04 ± 0.11	1.04 ± 0.05
97.4	31665 ± 1028	31657 ± 251	0.89 ± 0.09	0.88 ± 0.06

The piezoelectric effect observed in this work stems from all three terms on the right side of Eq. (8). Both the change in κ with stress (Fig. 5 and Table 1) and the change of the stored charge Q with stress contribute to the effect. The change of Q dominates, though all three terms contribute comparably. The total d is the sum of the contributions from the three terms on the right side of Eq. (8). Hence, the total d is $(3.9 \pm 0.6) \times 10^{-8}$ pC/N and $(4.8 \pm 0.5) \times 10^{-8}$ pC/N for type A fiber and type B fiber, respectively. This means that the total d is essentially equal for the two types of fiber. These values are smaller by orders of magnitude than those of well-known piezoelectric ceramics and polymers.

Stresses that are much higher than those of this work are possible, due to the high tensile strength of the carbon fibers. Extrapolation of the curve of electric field vs. stress (Fig. 6(a)) suggests that, at the stress equal to the tensile strength, the electric

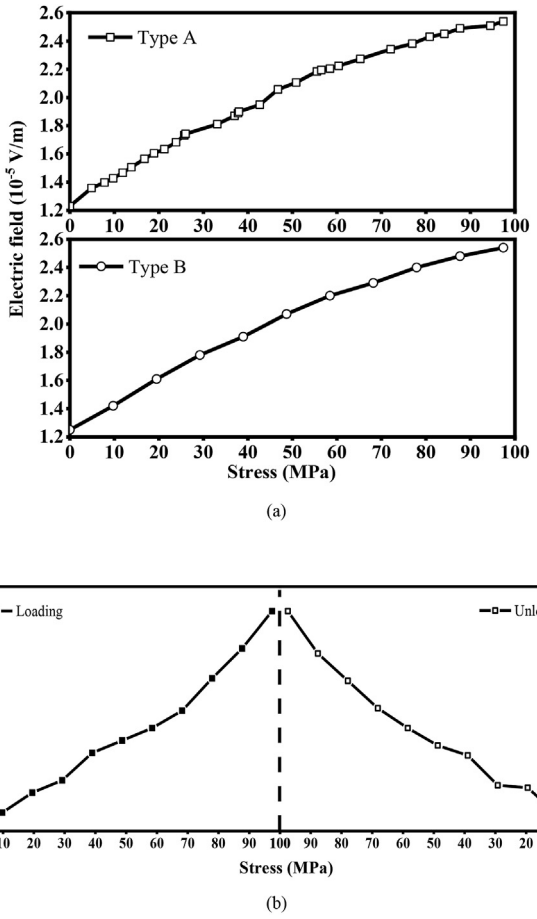

Fig. 6. Effect of tensile stress on the electric field output. The specimen length between the two electrodes is 95.25 mm for both type A fiber and type B fiber. (a) Electric field output during loading for type A and B fiber. (b) Comparison of the effect during loading (left panel) and subsequent unloading (right panel) for type A fiber.

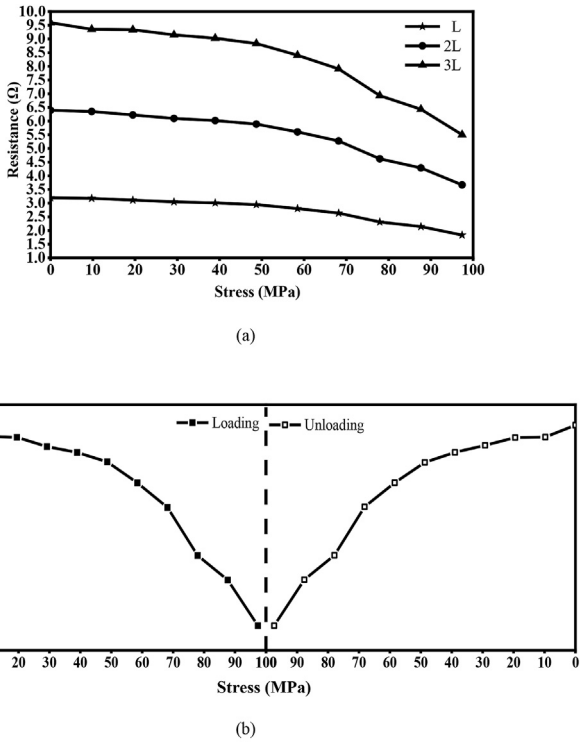

Fig. 7. Effect of tensile stress on the measured resistance R_m of type A fiber. (a) Resistance during loading of carbon fiber tow of lengths L, 2L and 3L. (b) Comparison of the effect during loading (left panel) and subsequent unloading (right panel). The specimen length between the two electrodes is 95.25 mm.

field output is 6.2×10^{-4} V/m. The use of electrical contacts that are 1 m apart (as is made possible by the large size of a composite structure) would give a voltage up to 0.62 mV only.

The electrical energy output of the piezoelectric effect of unmodified carbon fiber is too small for use in large-scale mechanical energy harvesting. Nevertheless, it is useful for providing piezoelectricity-based stress sensing, as shown by Fig. 3 in terms of capacitance-based stress sensing, and by Fig. 6 in terms of voltage-based stress sensing, thereby enabling the carbon fiber and its structural composites to be self-sensing. Capacitance-based self-sensing is more attractive than voltage-based self-sensing, because capacitance measurement does not require an intimate electrical contact between the electrode and the specimen surface, whereas voltage measurement does. In case of a composite material with a paint coating, the paint can serve as the dielectric film for capacitance measurement, whereas it needs to be removed prior to the application of the electrodes for voltage measurement.

Damage sensing is to be distinguished from strain/stress sensing. Defects such as microcracks tend to impede current flow, thereby increasing the resistivity and decreasing the permittivity. This research group has previously reported capacitance-based damage sensing in continuous carbon fiber polymer-matrix composite [20]. The capacitance-based damage sensing also stems from the piezoelectric effect, since damage affects the piezoelectric coupling coefficient and the permittivity.

Fig. 7 shows that the measured resistance R_m decreases monotonically with increasing stress during loading, whether the carbon fiber tow is of length L, 2L or 3L. The resistance change is totally reversible upon unloading.

For every stress value, the plot of R_m vs. distance l according to Eq. (7) is highly linear. Fig. 8 gives representative plots. The error in the resistivity ρ is obtained by considering the range of values of the slope.

Fig. 9 and Table 1 show that the resistivity decreases monotonically with increasing stress. The reversibility of the resistivity decrease is supported by the reversibility of the resistance decrease (Fig. 7(b)). The resistivity decreases by up to 43% and 44% for type A fiber and type B fiber, respectively. This means that the fractional decrease in resistivity due to the stress is essentially equal for the two types of fiber. This decrease is attributed to the increase in the degree of preferred orientation of the carbon layers along the fiber axis as the tensile stress increases. The enhancement of the preferred orientation of carbon fiber by the application of tensile stress (780 MPa, corresponding to a load of 5 g on a single fiber of diameter 9 μm and modulus 380 GPa) has been previously reported, as supported by the results of X-ray diffraction [17]. Consistent with the increase in the preferred orientation is the modulus increase as the stress increases [17–19].

The decrease of the resistivity with increasing tensile stress (up to a strain of 0.041%) (Fig. 9) is a negative piezoresistive effect. Negative piezoresistivity has been previously reported in carbon fibers [5,8–11]. As shown in Fig. 9, the resistivity decreases monotonically with increasing stress/strain. The behavior is similar for type A fiber and type B fiber.

Due to the very high resistivity anisotropy of a graphite crystallite, the degree of preferred orientation of the carbon layers in a carbon fiber is the main factor in affecting the axial resistivity of the fiber. The resistivity decrease is thus attributed to the increase in

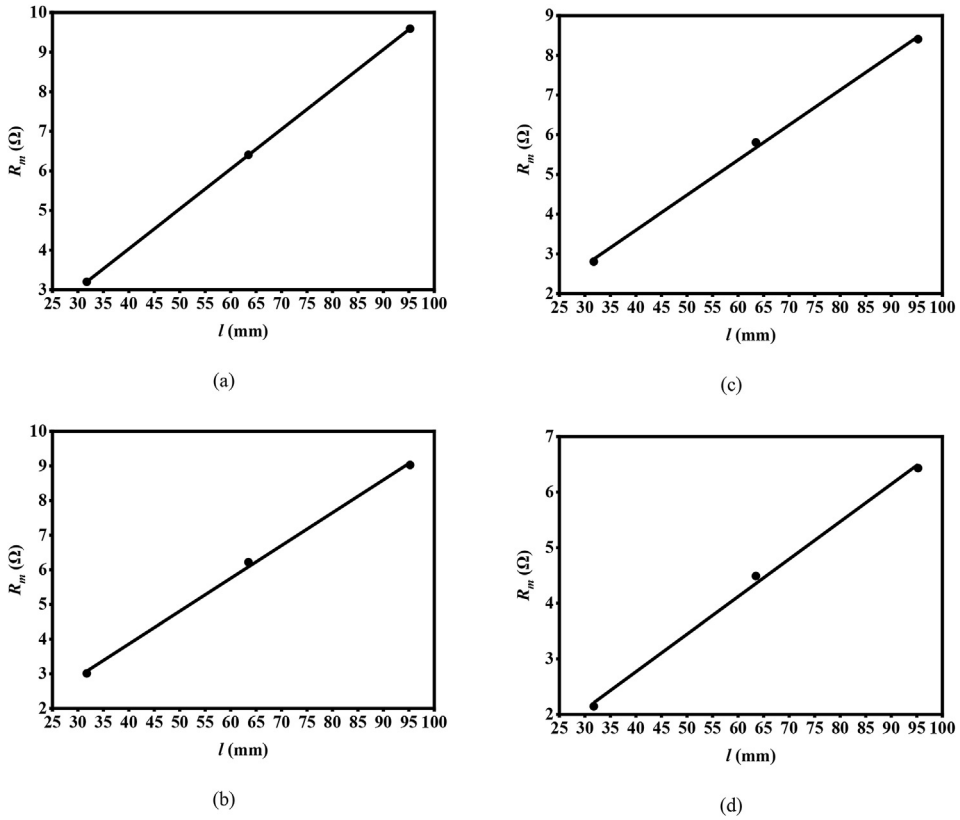

Fig. 8. Plot of R_m vs. distance l according to Eq. (7) for type A fiber. (a) Stress = 0. (b) Stress = 39.0 MPa. (c) Stress = 58.4 MPa. (d) Stress = 87.7 MPa.

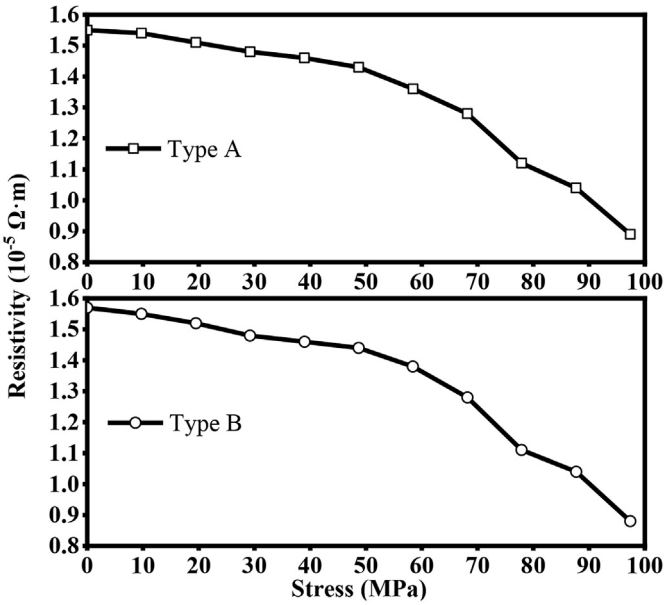

Fig. 9. Effect of the tensile stress on the electrical resistivity (DC) of carbon fiber during loading.

the preferred axial orientation of the carbon layers as the stress/strain increases. The elastic modulus is another material property that is known to increase with increasing degree of preferred orientation of the carbon layers. The above elucidation of the scientific origin of the resistivity decrease is consistent with the previous reports that the elastic modulus of PAN-based carbon fibers increases with increasing tensile stress [17–19]. The negative slope of the plot of resistivity vs. stress increases in magnitude as the stress increases. In other words, the resistivity decrease is slight at low stress/strain and significant at high stress/strain. According to Fig. 9, a minimum stress of 50 MPa is needed in order for the piezoresistive effect to reach a high degree. This trend means that the effect of stress on the preferred orientation is more significant when the stress is higher, as expected from the fact that the stress must be adequate in order to enhance the preferred orientation. This interpretation of the resistivity decrease is supported by the slight increase in the modulus as the stress increases, as shown in Fig. 2 and as previously reported [17–19].

The trend for the resistivity decrease upon tensile stress application (Fig. 9) is similar to that for the permittivity increase upon tensile stress application (Fig. 5). The positive slope of the plot of the relative permittivity vs. stress increases in magnitude as the stress increases. In other words, the permittivity increases slightly with increasing stress at low strains and increases more significantly at high strains. A minimum stress of about 80 MPa is needed in order for the permittivity increase upon stress increase to be significant. Due to the concomitant decrease of the resistivity with stress, this dependence of the permittivity on stress is at least partly due to the increase in the preferred orientation of the carbon layers as the stress increases. The permittivity of a graphite crystallite is expected to be anisotropic, though it has not been reported. On the other hand, the anisotropy of the permittivity of the longitudinal and transverse directions of a unidirectional carbon fiber polymer-matrix composite has been previously reported [20]. As shown for the unidirectional carbon fiber polymer-matrix composite, the resistivity anisotropy (1500) is much greater than the permittivity anisotropy (1.3) [20]. Therefore, the permittivity anisotropy of a graphite crystallite is likely lower than the corresponding resistivity

anisotropy. As a consequence, the resistivity is more sensitive to the preferred orientation than the permittivity. This difference probably contributes to the minimum stress for significant permittivity increase to be greater than the minimum stress for significant resistivity decrease.

The curve of the resistivity vs. stress (Fig. 9) can be approximated as consisting of two linear regimes. For the low-stress regime (stress ranging from 0 to 50 MPa), $\delta\rho/\rho = -0.0806$ and -0.0828 for type A fiber and type B fiber, respectively, and $\delta\ell/\ell$ = stress/modulus = 50 MPa/240 GPa = 0.0208% for both type A and type B fibers. Hence, based on Eq. (1), $\delta R/R = -0.0803 \pm 0.0024$ and -0.0825 ± 0.0041 for type A fiber and type B fiber, respectively. Thus, for the low-stress regime, the gage factor is -386 ± 10 and -406 ± 20 for type A and type B fibers, respectively. This means that the gage factor in the low-stress regime is essentially equal for the two types of fiber. For the high-stress regime (stress ranging from 50 to 100 MPa, and corresponding strain relative to the value at 50 MPa), $\delta\rho/\rho = -0.3814$ and -0.3889 for type A fiber and type B fiber, respectively, and $\delta\ell/\ell$ = stress/modulus = (100–50) MPa/240 GPa = 0.0208% for both type A and type B fibers. Hence, based on Eq. (1), $\delta R/R = -0.3811 \pm 0.0471$ and -0.3886 ± 0.0285 for type A fiber and type B fiber, respectively. Thus, for the high-stress regime, the gage factor is -1830 ± 226 and -1914 ± 140 for type A fiber and type B fiber, respectively. This means that the gage factor in the high-stress regime is essentially equal for the two types of fiber.

All of the above values of the gage factor are very high in magnitude and allow resistance-based stress self-sensing. Such a large magnitude of the negative gage factor has not been previously reported for any carbon fiber, as discussed in the Introduction.

The large magnitude of the gage factor is partly due to the strain dependence of the gage factor, i.e., the gage factor increasing with increasing strain, as explained below. It has been previously reported that the gage factor decreases with increasing strain for high-modulus carbon fiber (modulus = 786 GPa), whereas it is independent of the strain for low-modulus carbon fiber (modulus = 330 GPa) [7,8]. The strain dependence of the gage factor for this high-modulus fiber is attributed to the high inherent degree of preferred orientation and the resulting increasing difficulty of increasing this degree as the strain increases [7,8]. In this work, a low-modulus fiber with modulus (240 GPa) even lower than the value of 330 GPa for the low-modulus fiber of the prior work [7,8] is used, and the gage factor increases with increasing strain. This is because the positive effect of the strain on the degree of preferred orientation increases with increasing strain in a fiber of such low modulus. Therefore, it appears that the lower is the modulus, the greater is the tendency for the gage factor to increase with increasing strain. In other words, the higher is the modulus, the greater is the tendency for the gage factor to decrease with increasing strain. Thus, the observation in this work that the gage factor increases with increasing strain is in line with the observations of prior work [7,8] for fibers with higher values of the modulus.

It should be noted that the prior work [7,8] used relatively high strains (ranging from 1×10^{-3} to 7×10^{-3}) compared to the strain range of this work. Carbon fiber is a brittle material. The higher is the strain, the more is the tendency for damage in the fiber. Damage (such as microcracks) would increase the resistivity, thereby reducing the extent of negative piezoresistivity. Indeed, the gage factor of +1.9 for carbon fiber in the very-high-stress regime (strain ranging from 4×10^{-3} to 1.1×10^{-2}) corresponds to a situation that involves a degree of fiber damage, as indicated by a degree of irreversibility of the resistance increase (i.e., the resistance not returning to the initial value upon unloading) [9]. The higher is the strain amplitude, the more is the degree of irreversibility of the resistance change [9]. In order to observe the strong negative piezoresistivity, the strain must be kept low (below 0.4%, preferably below 0.041%), i.e., the stress must be kept low (below 1 GPa, preferably below 100 MPa).

Although the fractional decrease in the resistivity (up to 43% and 44% for type A fiber and type B fiber, respectively) due to the stress is low compared to the fractional increase in the permittivity (up to 150% for both type A fiber and type B fiber) due to the stress, it is significant. The permittivity and resistivity are not independent, according to the Kramers-Kronig Relationship [21]. Lower resistivity due to greater preferred orientation enables larger excursion of the charge carriers (electrons and/or holes) during polarization, thereby resulting in higher permittivity. Thus, the increase in permittivity due to the stress is at least partly associated with the decrease in resistivity due to the stress.

Table 2 compares the electromechanical behavior of type A and type B fibers. Type B may be slightly stronger in the piezoelectric and piezoresistive behavior than type A, as indicated by the piezoelectric coupling coefficient and gage factor. However, with consideration of the errors, the difference is negligible. This means that the sizing and the number of fibers per tow have little (if any) influence on the piezoelectric and piezoresistive behavior. This in turn means that the fiber-fiber interaction plays little role, if any, in affecting the reported behavior.

The negative piezoresistivity reported here is to be distinguished from that previously reported for continuous carbon fiber polymer-matrix composites [22]. The previously reported negative piezoresistivity is associated with the increase of the through-thickness resistivity upon longitudinal tension and decrease in the through-thickness resistivity upon longitudinal compression, as caused by the decrease in the degree of contact between fibers of adjacent laminae upon longitudinal tension [22].

4. Conclusion

This work reports the piezoelectric and piezoresistive behavior

Table 2
The piezoelectric coupling coefficient d_{33} and piezoresistive gage factor of type A and type B carbon fibers. The strain range (calculated based on the measured modulus given in Fig. 2) is that for obtaining the slope of the associated curve.

Phenomenon	Property	Type A fiber		Type B fiber	
		Value	Strain (%) range	Value	Strain (%) range
Direct piezoelectric	d_{33} (pC/N), Eq. (10),[a]	$(+1.7 \pm 0.3) \times 10^{-8}$	0.004–0.024	$(+2.1 \pm 0.2) \times 10^{-8}$	0.004–0.024
Direct piezoelectric	d_{33} (pC/N), Eq. (11),[b]	$(+1.3 \pm 0.2) \times 10^{-8}$	0.008–0.033	$(+1.8 \pm 0.3) \times 10^{-8}$	0.008–0.033
Direct piezoelectric	d_{33} (pC/N), Eq. (12),[b]	$(+9.3 \pm 0.6) \times 10^{-9}$	0.008–0.033	$(+8.6 \pm 0.5) \times 10^{-9}$	0.008–0.033
Direct piezoelectric	d_{33} (pC/N), total[c]	$(+3.9 \pm 0.6) \times 10^{-8}$	0.004–0.033	$(+4.8 \pm 0.5) \times 10^{-8}$	0.004–0.033
Piezoresistivity	Gage factor[d]	-386 ± 10	0–0.021	-406 ± 20	0–0.021
		-1830 ± 226	0.021–0.042	-1914 ± 140	0.021–0.042

[a] Obtained from the slope of the main linear region (strain range shown) of the curve of the electric field vs. stress.
[b] Obtained from the slope of the main linear region (strain range shown) of the curve of the relative permittivity vs. stress.
[c] The total value is the sum of the values based on Eqs. (10)–(12).
[d] Obtained from the slope of the main linear region (strain range shown) of the curve of resistivity versus stress.

of unmodified continuous carbon fiber. Not needing modification means that the technology can be implemented to existing structures that do not have the modification. In addition, the first report of the effect of stress on the permittivity of carbon fiber is provided. All the effects are along the fiber axis. The stress is tensile in the elastic region (strain $\leq$0.041%, stress $\leq$100 MPa). All three effects enable the carbon fiber to be self-sensing, as demonstrated in this work. The piezoelectric effect enables capacitance-based and electric-field-based self-sensing; the piezoresistivity enables resistance-based self-sensing; the effect of stress on the permittivity enables capacitance-based self-sensing.

The piezoelectric behavior is the direct piezoelectric effect, which occurs without the need for electric poling. The effect is attributed partly to the increase in stored charge and partly to the increase in permittivity with increasing stress. This increase in permittivity is accompanied by a decrease in resistivity, as both effects result from the increased movement of the charge carriers. The increased charge carrier movement is due to the enhanced preferred orientation of the carbon layers along the fiber axis as the stress increases.

The carbon fiber is PAN-based, with tensile modulus 240 GPa, diameter 7.0 μm, and density 1.77 g/cm^3. The electrical resistivity is $1.6 \times 10^{-5}\,\Omega$ m in the absence of an applied stress. Two types of fiber (type A and type B) that differ in the sizing (in both sizing composition and sizing amount) and the number of fibers per tow are comparatively studied. The comparative study indicates that the sizing, number of fibers per tow and fiber-fiber interaction have negligible effect, if any, on the electrical, mechanical and electromechanical behavior.

The piezoelectric behavior pertains to the capacitance and DC electric field output increasing monotonically and reversibly with increasing tensile stress/strain for strains (elastic region) up to 0.041% for both type A and type B fibers. The increase in C_m is due to the increase in the relative permittivity κ. The electric field output increase due to the stress is up to 110% and 103% for type A fiber and type B fiber, respectively. For type A fiber, the piezoelectric coupling coefficient d is low, at $(+3.9 \pm 0.6) \times 10^{-8}$ pC/N, of which $(+1.7 \pm 0.3) \times 10^{-8}$ pC/N is contributed by the increase in electric field output, $(+1.3 \pm 0.2) \times 10^{-8}$ pC/N is contributed by the relative permittivity increase, and $(+9.3 \pm 0.6) \times 10^{-9}$ pC/N is contributed by the electric field output and relative permittivity increase in combination. For type B fiber, d is also low, at $(+4.8 \pm 0.5) \times 10^{-8}$ pC/N, of which $(+2.1 \pm 0.2) \times 10^{-8}$ pC/N is contributed by the increase in electric field output, $(+1.8 \pm 0.3) \times 10^{-8}$ pC/N is contributed by the relative permittivity increase, and $(+8.6 \pm 0.5) \times 10^{-9}$ pC/N is contributed by the electric field output and relative permittivity increase in combination. In spite of the low d value, the piezoelectric behavior allows stress self-sensing, with the stress indicated by either the voltage (electric field) or the capacitance. Accompanying this behavior is that the relative permittivity (2 kHz) increases (by up to 153%, up to 31665, for type A fiber, and by up to 152%, up to 31657, for type B fiber) and the DC resistivity decreases (by up to 43%, down to $8.9 \times 10^{-6}\,\Omega$ m, for type A fiber, and by up to 44%, down to $8.8 \times 10^{-6}\,\Omega$ m, for type B fiber) monotonically and reversibly with increasing stress/strain in the same range.

The decrease of the resistivity with increasing stress corresponds to strong negative piezoresistivity, which is attributed to the increase in the preferred orientation of the carbon layers along the fiber axis as the stress increases. For type A fiber, the gage factor is -386 ± 10 at strains ranging from 0 to 0.021% and is -1830 ± 226 at strains ranging from 0.021% to 0.042%. For type B fiber, the gage factor is -406 ± 20 at strains ranging from 0 to 0.021% and is -1914 ± 140 at strains ranging from 0.021% to 0.042%. The high magnitude of the negative gage factor for both strain ranges and for both fiber types is attributed to (i) the low modulus (240 GPa), the associated relatively low degree of preferred orientation, and the consequent feasibility of increase in the degree of preferred orientation as the strain/stress increases, and (ii) the low strains used and the tendency for relatively high strains (as used in prior work [9]) to cause a degree of damage that would increase the resistivity, thereby reducing the extent of negative piezoresistivity.

The piezoelectric and piezoresistive effects also allow damage sensing (not investigated in this work), due to the expected effects of damage on the piezoelectric coupling coefficient, permittivity and resistivity. Capacitance-based damage sensing has been previously shown in the in-plane directions of a continuous carbon fiber polymer-matrix composite [20] without investigation of the piezoelectric behavior. Resistance-based damage sensing has been previously shown by the irreversible resistance increase in carbon fiber [9] and continuous carbon fiber polymer-matrix composites [1].

References

[1] D.D.L. Chung, Processing-structure-property relationships of continuous carbon fiber polymer-matrix composites, Mater. Sci. Eng. R 113 (2017) 1–29.
[2] N. Masghouni, J. Burton, M.K. Philen, M. Al-Haik, Investigating the energy harvesting capabilities of a hybrid ZnO nanowires/carbon fiber polymer composite beam, Nanotechnology 26 (9) (2015) 95401.
[3] V. Kostopoulos, P. Tsotra, P. Karapappas, S. Tsantzalis, A. Vavouliotis, T.H. Loutas, A. Paipetis, K. Friedrich, T. Tanimoto, Mode I interlaminar fracture of CNF or/and PZT doped CFRPs via acoustic emission monitoring, Compos. Sci. Technol. 67 (5) (2007) 822–828.
[4] F. Mischok, O. Durieux, Y. Vagapov, D. Fedyashin, Practical characterisation of the piezo electric properties of a 3K T300 carbon fibre for impact sensoring, in: Proc. IEEE Int. Conf. of Russian Young Researchers in Electrical and Electronic Engineering (EIConRus), Moscow, Russia, 29 Jan - 1 Feb, 2018, pp. 1757–1760, https://doi.org/10.1109/EIConRus.2018.8317446.
[5] P.C. Conor, C.N. Owston, Electrical resistance of single carbon fibers, Nature (London) 223 (5211) (1969) 1146–1147.
[6] D.D.L. Chung, Functional Materials, World Scientific, 2010. Chapters 2 and 3.
[7] C.A. Berg, H. Cumpston, A. Rinsky, Piezoresistance of graphite fiber materials, Fibre Sci. Technol. 4 (1971) 153–158.
[8] C.A. Berg, H. Cumpston, A. Rinsky, Piezoresistance of graphite fibers, Textil. Res. J. 42 (8) (1972) 486–489.
[9] X. Wang, D.D.L. Chung, Electromechanical behavior of carbon fiber, Carbon 35 (5) (1997) 706–709.
[10] S. Blazewicz, B. Patalita, P. Touzain, Study of piezoresistance effect in carbon fibers, Carbon 35 (10–11) (1997) 1613–1618.
[11] Y. Yao, J. Luo, X. Duan, T. Liu, Y. Zhang, B. Liu, M. Yu, On the piezoresistive behavior of carbon fibers – cantilever-based testing method and Maxwell-Garnett effective medium theory modeling, Carbon 141 (2019) 283–290.
[12] https://www.teijincarbon.com/fileadmin/PDF/Datenbl%C3%A4tter_en/Filament-Product_programm__EU__v27_2018-06-27_EN.pdf (as viewed on Dec. 15, 2018).
[13] http://ase.au.dk/fileadmin/www.ase.au.dk/Filer/Laboratorier_og_vaerksteder/Komposit-lab/Fiber/Carbon/Carbon_UD_HS__194_gsm__Tenax-E_HTS45_E23_-_TDS.pdf (as viewed on Sept. 22, 2018).
[14] Xi X, Chung DDL. Colossal electric permittivity discovered in polyacrylonitrile (PAN) based carbon fiber, with comparison of PAN-based and pitch-based carbon fibers. (submitted).
[15] http://www.ykcomposites.com/SGL-Carbon-Fiber-Continuous-Filament-29.html (as viewed on Dec. 15, 2018).
[16] https://xdevs.com/doc/Keithley/2002/SPEC-2002.pdf (as viewed on Sept. 22, 2018).
[17] G.J. Curtis, J.M. Milne, W.N. Reynolds, Non-Hookean behaviour of strong carbon fibres, Nature 220 (1968) 1024–1025.
[18] M. Shioya, E. Hayakawa, A. Takaku, Non-Hookean stress-strain response and changes in crystallite orientation of carbon fibres, J. Mater. Sci. 31 (1996) 21–32.
[19] G. Zhou, J. Byun, S. Lee, J. Yi, W. Lee, S. Lee, B. Kim, J. Park, S. Lee, L. Ho, Nano structural analysis on stiffening phenomena of PAN-based carbon fibers during tensile deformation, Carbon 76 (2014) 232–239.
[20] A.A. Eddib, D.D.L. Chung, First report of capacitance-based self-sensing and in-plane electric permittivity of carbon fiber polymer-matrix composite, Carbon 140 (2018) 413–427.
[21] https://en.wikipedia.org/wiki/Kramers%E2%80%93Kronig_relations (as viewed on Sept. 7, 2018).
[22] S. Wang, D.D.L. Chung, Negative piezoresistivity in continuous carbon fiber epoxy-matrix composite, J. Mater. Sci. 42 (13) (2007) 4987–4995.